Fault Detection and Diagnosis of Induction Motors Using Motor Current Signature Analysis and a Hybrid FMM–CART Model

Manjeevan Seera, *Member, IEEE*, Chee Peng Lim, Dahaman Ishak, and Harapajan Singh

***Abstract*— In this paper, a novel approach to detect and classify comprehensive fault conditions of induction motors using a hybrid fuzzy min–max (FMM) neural network and classification and regression tree (CART) is proposed. The hybrid model, known as FMM–CART, exploits the advantages of both FMM and CART for undertaking data classification and rule extraction problems. A series of real experiments is conducted, whereby the motor current signature analysis method is applied to form a database comprising stator current signatures under different motor conditions. The signal harmonics from the power spectral density are extracted as discriminative input features for fault detection and classification with FMM–CART. A comprehensive list of induction motor fault conditions, *viz.*, broken rotor bars, unbalanced voltages, stator winding faults, and eccentricity problems, has been successfully classified using FMM–CART with good accuracy rates. The results are comparable, if not better, than those reported in the literature. Useful explanatory rules in the form of a decision tree are also elicited from FMM–CART to analyze and understand different fault conditions of induction motors.**

***Index Terms*— Classification and regression tree, fault detection and diagnosis, fuzzy min–max neural network, induction motor, motor current signature analysis.**

I. Introduction

MOTORS are commonly used devices to convert electrical energy to mechanical energy. In order to improve motor efficiency, variable speed drives are commonly used, and this has led to increased motor over-heating problems, harmonic problems, and shorter operational life of motors [1], [2]. As a result, effective fault detection and diagnosis techniques are needed in order to reduce the maintenance and downtime costs of motors. From the literature review, useful techniques for online detection and diagnosis of induction motor faults emerge rapidly, which are able to avoid unexpected failures of induction motors [1]. Examples include online condition monitoring techniques to observe motor parameters such as stator resistance and inductance [2], [3].

Manuscript received January 14, 2011; revised October 15, 2011; accepted October 16, 2011. Date of publication December 15, 2011; date of current version January 5, 2012. This work was supported in part by the Research University Grant of University of Science Malaysia under Grant 814089.

M. Seera and D. Ishak are with the School of Electrical and Electronic Engineering, University of Science Malaysia, Nibong Tebal 14300, Malaysia (e-mail: mseera@gmail.com; dahaman@eng.usm.my).

C. P. Lim is with the School of Computer Sciences, University of Science Malaysia, Pulau Pinang 11800, Malaysia (e-mail: cplim@cs.usm.my).

H. Singh is with the Faculty of Electrical Engineering, MARA University of Technology, Permatang Pauh 13500, Malaysia (e-mail: harapajan@gmail.com).

Digital Object Identifier 10.1109/TNNLS.2011.2178443

In general, fault detection and diagnosis techniques for electric motors are provided by some combination of mechanical and electrical condition monitoring methods. Whenever mechanical sensors are used to assess the health conditions of a machine, they normally are installed on some expensive or load-critical machines where the high cost of a continuous monitoring system can be justified [4]. Nevertheless, current monitoring can be implemented inexpensively on machines with arbitrary sizes by using current transformers. In this regard, effective and low-cost fault detection techniques can be implemented, hence saving the maintenance and downtime costs of motors. This is the reason why this paper focuses on motor current signature analysis (MCSA) for fault detection and diagnosis of induction motors.

Among different types of electric motors, induction motors contribute more than 60% of the electrical energy produced [5]. Induction motors are widely used in different areas, which include manufacturing machines, belt conveyors, cranes, lifts, compressors, trolleys, electric vehicles, pumps, and fans [6]. It has been reported [7]–[9] that shipment of AC motors and three-phase induction motors in Europe are at 96.2% and 87%, respectively. Failure surveys by electric power research institute [10], [11] show that the typical failure percentages of induction motors are as follows: stator-related faults 38%, rotor-related faults 10%, bearing-related faults 40%, and other faults 12%.

This paper aims to design and develop a low-cost and yet effective method to detect and classify comprehensive fault conditions of induction motors, as indicated in [10] and [11]. We select MCSA, which is a low-cost and convenient method, for fault detection and diagnosis in this paper. MCSA deploys the results of spectral analysis of the supply current to detect a particular motor failure in the drive system. There are also reports [12], [13] that focus on detecting mechanical faults of machines using MCSA, but most of the methods used ignore the load effects, or assume that the load is known [14]. An effective use of MCSA in fault detection of induction motors is to sample the harmonics components in the stator-current spectrum using the fast fourier transform (FFT) [11], [15]–[22]. FFT is a popular and useful technique for signal analysis, and is applied in this paper to process signals derived from stator currents for detecting and diagnosing induction motor faults under different load conditions.

Rule extraction plays an important role in fault detection and diagnosis systems. Rules provide explanation of the system

2162–237X/$26.00 © 2011 IEEE

predictions to users. In [23], the method for extracting fuzzy rules directly from numerical input-output data for pattern classification is presented while in [24], the method is extended for function approximation where each output variable is divided and each interval is treated as a class. In [25], rules for unbalanced supply, unbalanced mechanical load, encoder, and voltmeter failures are extracted from a neuro-fuzzy system. The rules provide some insight on how to avoid definitive damage or failure to AC motors. Sii *et al*. [26] developed a safety model based on fuzzy logic for maritime and offshore safety. The rules for personnel, organization, and environment consequences are evaluated using a Mamdani-type interference system to assess the risk level of the system. In [27], using radial basis function (RBF) with evolutionary programming, the classification rules for engine vibration analysis are found by examining the basis functions. It is reported in [28] that early detection of induction motor faults increases the safety of operators handling the machines, and the rules extracted from decision trees and adaptive neuro-fuzzy inference serve to achieve this purpose.

In this paper, the task of fault detection and diagnosis of induction motors using a hybrid model comprising the fuzzy min–max (FMM) [29] neural network (NN) and the classification and regression tree (CART) [30] is described. The hybrid model is known as FMM–CART. For the experimental study, MCSA is first applied to produce data features based on the power spectral density (PSD) of real stator-current signals of induction motors. Then, various types of fault conditions are classified using the FMM–CART model. In general, a number of NN models have been demonstrated to be useful for fault detection and diagnosis tasks. Examples include the use of recurrent NN model with back propagation (BP) [31] for detection of sensor and actuator faults of an attitude control subsystem of low-earth orbit satellites, and the use of the RBF model [32] for fault detection and diagnosis of a class of nonlinear systems with modeling uncertainties. In this paper, we focus on the FMM model because of its one-pass training with online learning capabilities, as well as other advantages as explained in [29]. However, similar to many other NN models (e.g., [31], [32]), FMM does not have the capability of producing rules to explain its predictions, which is very important in fault detection and diagnosis tasks. On the other hand, while CART has the capability of explaining its prediction with rules, it is less flexible in terms of learning from data samples. The hybrid model, FMM–CART, overcomes the limitations of both FMM and CART by having an intelligent learning system that is able to learn from data samples, and, at the same time, to produce rules for explanation of its predictions.

Here, we demonstrate that FMM–CART is capable of detecting and diagnosing comprehensive induction motor faults, with explanatory rules to justify its predictions. While other reports in the literature mainly cover one or two inductor motor faults (e.g., [11], [24], [33], [34], as well as others in Section II), and/or use information from more than one source, e.g., stator currents and vibration signals (e.g., [16], [17], [28], [35], as well as others in Section II), FMM–CART, on the other hand, is a low-cost system which exploits information coming from only one source, that is, stator currents using MCSA, for detection and diagnosis of a comprehensive list of induction motor faults, which include broken rotor bars, unbalanced voltages, stator winding faults, and eccentricity problems, as reported by electric power research institute [10], [11]. The results of FMM–CART are better than those of FMM or CART individually, as well as those from other NN-based and non-NN-based methods reported in the literature.

The organization of this paper is as follows. In Section II, a review on motor fault detection and diagnosis is presented. In Section III, a number of fault conditions of induction motors used in this paper are described. The methods used for analysis are explained in Section IV. The results and discussion are included in Section V. Finally, concluding remarks are given in Section VI.

II. Review of Motor Fault Detection and Diagnosis Methods

In this section, a variety of motor fault detection and diagnosis methods based on computational intelligence and statistical models are reviewed. The review is sorted by information from either single or multiple sources, which is further divided into single or multiple faults, as follows.

A. Information from Single Source

A review on motor fault detection and diagnosis based on information coming from single source, primarily either electrical or mechanical, is presented, as follows.

1) Single Fault: BP is a common supervised learning method for feed-forward NNs [18]. Current signals were transformed to magnitudes using FFT, and side-band frequency magnitudes were fed into a feed-forward NN trained with BP to detect broken rotor bars [18]. Sadeghian *et al*. [36] used stator-current signals as a source for detecting broken rotor bars. An algorithm using wavelet packet decomposition (WPD) was applied to analyze the signals. Multiple frequency resolutions were generated and fed into a multiLayer perceptron (MLP) network for fault classification. In [19] and [37], stator-current signals were employed as inputs for detection of broken rotor bars. Ayhan *et al*. [37] used multiple discriminant analysis (MDA) as a classifier to detect broken rotor bars. Guo *et al*. [19] used Park's Vector modulus to avoid the characteristic components from being submerged by fundamentals in the spectrum of stator line current. The resulting output was fed into a fuzzy wavelet NN for fault detection and classification of broken rotor bars.

In [38], vibration signals were used as inputs to an improved distance evaluation technique where the most important features were extracted from the original feature set. The features were used by an adaptive neuro-fuzzy inference system (ANFIS) model to detect rolling element bearing failures. Zhang *et al*. [39] performed bearing fault diagnosis with the multiscale entropy method using vibration signals. Calculation of entropies across a sequence of scales, which considered dynamic nonlinearity and coupling effects between mechanical components, was accomplished, and an ANFIS model was

then used for fault classification [39]. Hwang *et al*. [40] used motor vibration signals to obtain the corresponding cepstrum coefficients, which were then used for motor bearing fault detection with a NN trained with BP. In [41], a Concordia transform-based algorithm, where a 2-D representation could be formulated from three-phase current signals, was first used. The outputs were then fed to a RBF NN for detection of bearing defects. In [42], classification features were extracted from raw vibration signals, and then fed into the modified distance discrimination technique where some salient features were selected from the original feature set. The selected feature set was supplied to an improved fuzzy ARTMAP network for detection of rolling element bearing faults. Samanta and Nataraj [43] analyzed time domain vibration signals for feature extraction. The features extracted from the original and processed signals were used as inputs to a particle swarm optimization model. The resulting output was used by a proximal support vector machine (SVM) for detection of defective bearings.

2) Multiple Faults: Rodríguez *et al*. [11] used a predictive filter to separate the fundamental from harmonic components of current signals, and a fuzzy model to detect broken rotor bars and inter-turn stator winding faults of induction motors. Lee *et al*. [33] used Fourier and wavelet transformations to obtain the sideband and detail value characteristics of different motor conditions. The results were used by a dynamical polynomial NN for classification of broken rotor bar, bowed rotor, faulted bearing, and eccentricity faults. Three-phase stator-current signals were used to form input features using principal component analysis (PCA) for detection and classification of stator winding inter-turn short and eccentricity faults, and an RBF-based MLP network was used for classification [44]. Widodo and Yang [34] used start-up transient currents processed with PCA as useful features for detection of unbalanced phase, eccentricity, and bearing failures with a wavelet-based SVM. In [45], eigenvector/eigenvalue analysis based on stator currents was performed for detection of broken rotor bar and stator winding faults. The fault severity was reported according to the relationship between the eigenvectors and eigenvalues of the reference stator currents. The short-time Fourier transform was deployed to process the quasi-steady vibration signals to continuous spectra for use of a NN trained with Levenberg–Marquardt [46]. Air-gap eccentricity and broken rotor bars were detected from changes in the expectation of vibration spectra modeling error.

Nguyen *et al*. [47] used vibration signals for detection of damaged bearing and rotor unbalance. A genetic algorithm (GA) with decision tree and multiclass SVM were applied to increase the efficiency of selection method for fault classification. Cho *et al*. [48] used current signals for detection of faulty stator and bearing. Fault classification was accomplished using a dynamic Bayesian network with simultaneous perturbation stochastic approximation [48].

B. Information from Multiple Sources

A review on motor fault detection and diagnosis based on information coming from multiple sources, which include electrical, mechanical, and thermal, is presented, as follows.

1) Single Fault: Liu *et al*. [49] deployed both currents and vibration signals to classify broken rotor bars. A fusion between fuzzy measures and fuzzy integrals was employed for fault classification. In [20], diagnostic features were extracted from current and voltage measurements, and the most relevant features were selected based on the k-nearest neighbors rule for classification. Then, fault classification of broken rotor bars with a Kalman algorithm [20], which allowed predicting the evolution of the partially known modes, was conducted. Bouzid *et al*. [50] monitored three-phase shifts between the line current and the phase voltage of machines. Then, an MLP trained with BP was used for detection of inter-turn short-circuit faults. Taplak *et al*. [51] measured amplitude, velocity, and acceleration values as vibration parameters as inputs to a feed-forward NN trained with BP for detection of bearing faults.

2) Multiple Faults: Han *et al*. [35] used three-phase stator currents and vibration signals for detection of unbalanced phase and eccentricity problems. The inputs were fed into a GA for feature reduction and NN tuning. Then, an adaptive resonance theory (ART)-Kohonen network was used for fault classification. In [28], Tran *et al*. used both vibration and current signals as inputs to detect rotor faults, eccentricity, and bearing faults. A decision tree was used as a feature selection procedure to select important features from the data set. The crisp rules obtained from the decision tree were converted to fuzzy if–then rules to identify the structure of ANFIS. In [17], different inputs, that is, voltage, current, speed, vibration, temperature, were used for detection of supply unbalanced, over/under voltage, and bearing faults. The inputs were processed with FFT and then fed into an MLP network trained with BP for fault classification. Ballal *et al*. [16] used five different inputs to an ANFIS model, that is, current, rotor speed, winding temperature, bearing temperature, and motor noise. The current signals were fed into FFT to process the fundamental and harmonic components. These harmonics, together with the remaining four inputs, were then fed into ANFIS for detection of inter-turn insulation failure and bearing wear of induction motors.

A fusion approach using classifier selection and decision fusion [52] was applied to detection of bearing failures, eccentricity, and unbalanced rotor faults in induction motors based on current and vibration signals. The fusion system was based on majority voting, Bayesian belief, multiagent, and modified Borda count. Liu *et al*. [49] deployed both currents and vibration signals to classify broken rotor bars and faulty bearings. A fusion between fuzzy measures and fuzzy integrals was employed for fault classification [49].

C. Review Summary

Based on the review, it can be seen that a comprehensive study that covers most of the common induction motor faults as reported in electric power research institute [10], [11] and with information coming from single input source is needed. Thus, a low-cost system with information only from

stator currents using MCSA for detection and diagnosis of comprehensive induction motor faults, which include broken rotor bars, unbalanced voltages, stator winding faults, and eccentricity problems, is developed and evaluated in this paper.

III. Fault Conditions of Induction Motors

An induction motor is one of the simplest and most rugged electric motors. It consists of two main parts, the stator and the rotor assemblies. The stator consists of wound poles that use the supply current to induce a magnetic field of the rotor using electromagnetic induction [53]. Comparatively, other motors require currents to be supplied directly to the rotor.

In this section, individual faults covered in our experimental study are explained. Induction motors are available in either single phase or three phase. In our experimental study, three-phase induction motors are deployed. Failure surveys [10], [11] by the Electric Power Research Institute indicate that induction motor faults (sorted from the most common faults) are as follows: bearing-related faults 40%, stator-related faults 38%, other faults 12%, and rotor-related faults 10%. In this paper, all these fault conditions are covered, whereby we treat unbalanced voltages as other faults.

A. Broken Rotor Bars

Two different types of cage rotors exist in induction motors, *viz.*, cast and fabricated. Cast cage rotors are used in motors up to 3000 kW rating while fabricated cages are found in motors of higher ratings, and are used in special machines. Cast rotors are almost impossible to get fixed once there are breakages or cracks in them, although they are more durable and rugged than fabricated cages [53]. During the broken rotor bars event, the sideband currents are given by [15]

$$f_b = (1 \pm 2ks)\, f \tag{1}$$

where $k = 1, 2, 3$, s is the slip, and f the supply frequency. When there are broken rotor bars, other frequency spectrums besides the fundamental ones, which can be observed from the stator-current spectrum, are given by [15]

$$f_b = \left[\left(\frac{k}{p}\right)(1-s) \pm s\right] f \tag{2}$$

where f_b are detectable broken bars frequencies, p is the number of pole pairs, and $k/p = 1, 2, 3$.

Broken rotor bars will not cause immediate failures of an induction motor. But, if there are many broken rotor bars, the motor may not be able to start once it is powered off. This is mainly due to insufficient accelerating torque during the start-up process.

B. Unbalanced Voltages

In a three-phase system, unbalanced voltages occur when the magnitudes of phase or line voltages are different. Unbalanced voltages shorten the life of a motor besides reducing the motor performance. Based on the National Equipment Manufacturer Association (NEMA) standard [54], once unbalanced voltages reach 5%, the temperature in the stator windings begins to rise, which eventually may cause the winding insulation to melt.

C. Stator Windings

Usually, the cause of stator winding faults is short circuits between a phase winding and the ground or between two phases [55]. Note that initial undetected turn-to-turn faults may gradually develop to a major short circuit, and may have a destructive effect on the stator coils.

Axial leakage flux from stator windings can be used to detect and locate stator inter-turns. The induced voltage in a search coil placed in the middle of the machine shaft is proportional to this flux component. The spectral constituents of this voltage are observed to detect a turn-to-turn fault [56]. These frequencies are given by

$$f_t = \left[k \pm \left(\frac{n}{p}\right)(1-s)\right] f \tag{3}$$

where $k = 1, 3$, $n = 1, 2, 3$, and p is the number of pole pairs.

Under the stator short circuit conditions, there are magneto-motive forces (MMFs) and flux density waves at all numbers of pole pairs and in both directions of rotation [57]. No new frequency components appear in the stator-current spectrum as a result of faults in the stator winding, and only a rise in the rotor slot harmonics can be expected. Any stator short circuit produces a negative sequence component in the input currents. During the event of a short circuit, the phase winding has less impedance, fewer turns, and less MMFs. This gives rise to a possibility of detecting stator short circuits by monitoring the amplitude of the phase currents [57].

D. Eccentricity Problems

Rotor eccentricity, which results in a nonuniform air gap, is divided into two categories: static and dynamic. Eccentricity-related faults commonly occur as a result of bearing faults [58]. In static eccentricity, the air gap has a fixed minimal position. This position rotates with the rotor in dynamic eccentricity. Due to imperfection in design and manufacturing procedures, up to 10% eccentricity is allowed [53]. Higher orders of eccentricity can cause rotor-to-stator rub, resulting in damage of rotor and/or stator windings or cores.

The presence of static and dynamic air gap eccentricity can be detected using MCSA. One of the equations describing the frequencies components is given by [59]

$$f_{ecc} = f_s \left[(kR \pm n_d)\frac{(1-s)}{p} \pm v\right] \tag{4}$$

where $n_d = 0$, in the case of static eccentricity, and $n_d = 1, 2, 3$, in the case of dynamic eccentricity, R is the number of rotor slots, s is the slip, and p is the number of pole pairs. In practice, both static and dynamic eccentricity coexists, and when this happens, low frequency components that are related to the rotation frequency do appear [55], as given by

$$f_e = f_s \pm f_r \tag{5}$$

where f_r is the rotational speed.

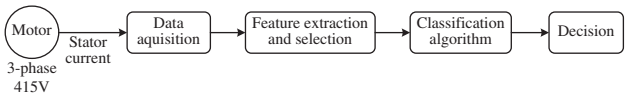

Fig. 1. Overview of the proposed method for fault detection and diagnosis.

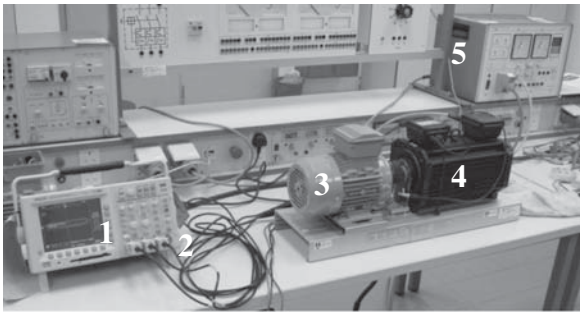

Fig. 2. Experimental study setup.

IV. Proposed Method for Fault detection and Diagnosis

In this section, the procedure from acquiring current signals from the motor to arriving at a decision on the potential motor faults is explained. A database comprising current signals from real experiments of fault detection and diagnosis of induction motors is established, as follows. The three-phase stator currents from an induction motor are measured using three current probes connected to an oscilloscope as a data acquisition unit. Data from oscilloscope are acquired using a network connection and are stored in a computer. A total of 10 cycles, equivalent to 0.2 s of the unfiltered three-phase stator currents, that is, phase A, phase B, and phase C, are transformed using FFT to the respective PSD for feature extraction. During feature extraction, selected pairs of harmonic magnitudes from the frequency spectrum are used as input features of FMM–CART. The output of FMM–CART is a prediction of five different motor conditions, that is, healthy (or fault-free) condition, broken rotor bars, unbalanced voltages, stator winding faults, and eccentricity problems. An overview of the proposed method for fault detection and diagnosis is shown in Fig. 1.

A series of experiments has been conducted using a laboratory-scale test rig. As shown in Fig. 2, the test rig consists of an oscilloscope (1), three current probes (2), an induction motor (3), a belt, shaft, a load inducer (4), and a load controller (5). A total of five 1 Hp, 415 V, 50 Hz, 4-pole induction motors were operated under various load conditions. Note that such an induction motor configuration is commonly found in many industrial applications [7]–[9]. For example, motors smaller than 10 Hp has a market share of 59.6% in Europe [7]. An assessment report in [9] indicates that 4-pole motors account for 70% of the total induction motors in Europe.

In this paper, a total of five induction motors were tested. One of the induction motors was in a healthy condition, which was used for comparison purposes with faulty motors. Other induction motors were operated with various fault conditions. First, induction motors having one and two broken bars in the rotor were tested. Next, the induction motor was operated by biasing one of three-phase unbalanced voltages by 5%, followed by 10%. Then, the induction motor was operated with 10% turn shorts in one of the three phases having stator windings short. Finally, 30% dynamic eccentricity and 10% static eccentricity were produced for experimentation. A number of tests were performed at 25%, 50%, 75%, and 100% load conditions. The load was electronically controlled, whereby the load conditions could be increased or decreased by turning the controller knob accordingly. Three AC probes were used to measure the stator currents, and the maximum measurement frequency was 50 kHz. A total of 10 000 data samples were captured at four different load conditions for each motor fault.

A. PSD

MCSA relies on the spectral analysis of the stator currents, or more precisely the supply currents of an induction motor, to detect an incipient motor fault. Spectral density methods are used to extract information from a signal and to describe the power distribution in the frequency domain. PSD is the Fourier transform of the autocorrelation function of a signal when the signal is stationary [60]. PSD is not restricted to using one specific harmonic for fault detection. From the literature, PSD has been used in motor imagery classification [60] as well as detection of broken rotor bars and shorted turns [1].

Computation of discrete data using a Fourier transform is called the discrete fourier transform (DFT). DFT transforms one function into another, and requires an input of a finite sequence of real or complex numbers. The FFT allows a fast computation of the Fourier coefficients. In this paper, FFT, instead of DFT, is used as it allows a faster computation. On the other hand, in classical Fourier analysis, the power of a signal can be obtained by integrating PSD, that is, the square of the absolute value of the Fourier-transform coefficients [60]. The values of the Fourier transform are in general complex quantities, where they contain both real and imaginary components. The square-amplitude of a complex number can be obtained by multiplying itself by its complex conjugate. In this paper, PSD is calculated by multiplying the FFT with its complex conjugates. It is then normalized by dividing it with the series length. The three-phase current signals are used to produce PSD for further analysis. PSD displays a 1000 Hz frequency spectrum which contains an odd number harmonics, ranging from the 1st to the 19th harmonic. These harmonics, which contain unique values for each condition, are fed to FMM–CART for fault detection and diagnosis.

B. FMM–CART Model

Simpson proposed two FMM models: one for pattern classification (a supervised learning model) [29] and another for pattern clustering (an unsupervised learning model) [61]. In addition to the original FMM networks from Simpson, variants of the FMM models have been proposed [62]–[65]. The general fuzzy min–max NN (GFMN) [62] combines both supervised and unsupervised learning paradigms into one

1. Load harmonics data set
2. Start FMM training process
   (a) Initialize all the minimum-maximum points
   (b) Identify the closest hyperbox to input pattern for expansion, if not, add a new hyperbox
   (c) Check if expansion caused any overlap between hyperboxes
   (d) If overlapping hyperboxes exist, contract the hyperboxes to eliminate the overlap
3. Use generated hyperboxes as CART inputs
   (a) Recursive splitting of nodes with each node assigned to a predicted class
   (b) Prune the tree using the cost-complexity method
   (c) Optimize the tree by calculating the misclassification rate
4. Use the final tree for fault classification

Fig. 3. Procedure of FMM–CART.

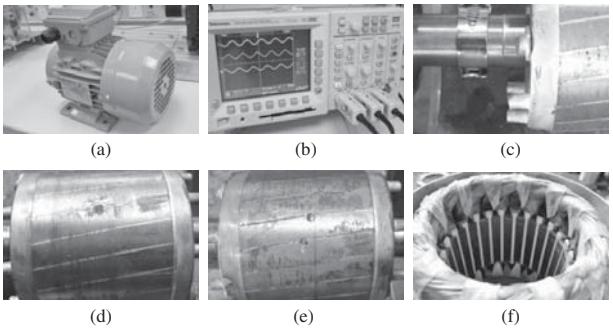

Fig. 4. Different conditions of the motor experiments conducted. (a) Healthy motor. (b) Unbalanced voltage. (c) Eccentricity. (d) One broken bar. (e) Two broken bars. (f) Stator winding fault.

learning algorithm. However, the learning algorithm needs a few passes of placing and adjusting hyperboxes in the pattern space. The fuzzy min–max NN classifier with compensatory neuron architecture (FMCN) [63] is a supervised classification model which eliminates the need of the contraction process as suggested by Simpson [29], [61] in solving the problem of overlaps in hyperboxes. However, when the compensatory hyperboxes become dominant, a smaller value of expansion coefficient is needed to achieve better performance [63]. The results for both GFMN [62] and FMCN [63] using benchmark data sets are discussed in Table I (Section V).

The granular reflex fuzzy min–max NN (GrRFMN) [64] uses hyperbox fuzzy sets to represent granular data, and a reflex mechanism structure to handle class overlaps. The GrRFMN has input nodes capable of processing granules in form of hyperboxes, which eliminates the need of double connections between the input and hyperbox nodes as in FMCN [63]. However, if data samples are less granulated, granulation and postprocessing may not be effective [64]. On the other hand, the monotone NN models [65] are designed to produce better accuracy and lower variance when compared to nonmonotone models. As explained in [65], the four-layer monotone NNs in combination with the min–max networks are capable of approximating continuous monotone function arbitrarily well. However, totally monotone prediction models depend monotonically on all variables in the input space, while partially monotone prediction models depend monotonically on some variables in the input space, but not all. In the experimental study (house pricing and Toyota car price prediction) [65], the partially monotone min–max networks are more accurate as compared with the totally monotone min–max networks and standard NNs, with the maximum average percentage error of 2.067%.

There are a number of advantages associated with the original supervised FMM network introduced by Simpson [29]. It possesses the capability of learning and adapting to new classes, while refining the existing classes quickly [29]. It is also simple and easy to use, and the training time is short as it only needs one pass to learn (compared to GFMN [62] that needs a few passes) and to refine its decision boundaries. As such, we focus on the original supervised FMM network in this paper, and we devise a hybrid model known as FMM–CART by combining FMM with CART.

In the experimental study, data samples used for FMM learning are taken from the PSD outputs. The hyperboxes of FMM (i.e., weights of FMM after training) form a crisp data set for tree building based on the CART procedure. The resulting tree is pruned into a simpler tree. Tree optimization is accomplished to ensure that there is no over-fitting. Then, the optimized tree is used for fault detection and classification. The procedure of FMM–CART is shown in Fig. 3, and is further explained as follows.

FMM constitutes the first part of FMM–CART. The supervised FMM network [29] is formed using hyperbox fuzzy sets. The size of a hyperbox is controlled by θ, which varies between 0 and 1. When θ increases from a small to a large value, the number of hyperboxes created is reduced. The membership function is set with respect to the minimum and maximum points of a hyperbox, and to the extent to which a pattern fits in the hyperbox. Further details of FMM can be found in [29].

The hyperboxes generated from FMM training serve as the input to CART [30] building. CART has the advantages of handling both numerical and categorical variables that are highly skewed. The structure of the tree does not change when any variable in its logarithm or root square values are replaced. The procedure of CART consists of three basic steps. The first step is tree building. A tree is built using recursive splitting of nodes, whereby a set of rules is established to split learning samples into smaller parts. Based on the decision matrix from the distribution of classes in the learning set, each resulting node is assigned a predicted class. The resulting tree consists of internal nodes and leaf nodes [66]. Tree pruning, the second step, is a sequence of simpler tree generation.

TABLE I
PERFORMANCE COMPARISON WITH FOUR UCI DATA SETS

Data	Iris		Wine		Ionosphere		Thyroid	
	Max	Min	Max	Min	Max	Min	Max	Min
GFMN	100.0	92.0	100.0	88.6	98.7	90.1	100.0	94.4
FMCN	100.0	98.0	100.0	100.0	100.0	96.0	100.0	98.1
FMM–CART	100.0	98.0	100.0	100.0	100.0	96.2	100.0	98.4

TABLE II
PERFORMANCE COMPARISON WITH THE IRIS DATA SET

Training set (%)	FMM—CART		FMCN		GFMN	
	LE (%)	TE (%)	LE (%)	TE (%)	LE (%)	TE (%)
35	1.58	5.63	1.85	6.25	5.50	9.37
45	0.21	5.34	0.00	6.17	8.69	11.11
50	0.00	3.62	0.00	4.00	1.33	6.66
60	0.00	2.67	0.00	3.33	1.10	5.00
70	0.00	2.05	0.95	2.22	7.61	8.88

LE – Learning error, TE – Testing error

Pruning the tree is necessary to improve the classification performance. The method of cost-complexity pruning [66] is used. It is based on a complexity parameter which is gradually increased during the pruning process. The final step consists of optimal tree selection. The data samples are divided into two subsets, one for learning which is used to split nodes and another for testing, which compares the misclassification rates for the subtrees. As the tree grows larger, the misclassification cost for the learning data decreases gradually. The final tree is then used for fault classification, in this case different induction motor faults. Further details on CART can be found in [30].

V. EXPERIMENTAL STUDY

In this section, the experimental study of FMM–CART is detailed. First, a performance comparison study is presented. Then, the effectiveness of FMM–CART for detecting and classifying individual and multiple faults in induction motors is evaluated.

A. Performance Comparison

Before going into the induction motor fault detection and diagnosis experiments, a performance comparison study between FMM–CART and two newer variants of FMM, *viz.*, GFMN [62] and FMCN [63], was first conducted. To have a fair comparison, the same testing procedure, whereby all samples were used for training and testing as reported in [63], was adopted, and four data sets from the University of California at Irvine (UCI) repository of machine learning, that is, Iris, Wine, Ionosphere, and Thyroid, were used. Table I summarizes the results of FMM–CART and those of GFMM and FMCN as reported in [63]. In general, GFMN yields the lowest results, while FMCN is slightly inferior in performance as compared with FMM–CART. Another performance comparison study with varying training sizes as reported in [63] was conducted. Using the Iris data set, the training set sizes varied from 35% to 70% of the total number of data samples, with the remaining as testing samples. The expansion coefficient was kept at $\theta = 0.2$. Table II shows the results of FMM–CART and the GFMN and FMCN results as reported in [63]. Again, FMM–CART exhibits the best results for all (except the learning error rate when the training set size $= 45$) settings.

B. Individual Induction Motor Faults

The experimental procedure started by acquiring current signals from induction motors with six different conditions as depicted in Fig. 4, that is, a healthy motor, motors with unbalanced voltages, eccentricity, one broken rotor bar, two broken rotor bars, and stator winding faults. Three-phase power was supplied to the induction motor and three current probes were clamped individually onto the cables of each phase. The current probes were connected to an oscilloscope where the current signals were captured. Current signals from the oscilloscope were transferred from the oscilloscope to the computer using a network connection. The current signals were transformed into their associated PSD. The PSD outputs comprised a 1000 Hz frequency spectrum, from the 1st to 19th harmonics. Note that in a balanced three-phase system, the triplen harmonic voltages should be absent. However, owing to machine supply and constructional unbalances, some of them may or may not be present in the motor supply currents [67]. To minimize the number of input features, the 3rd, 9th, and 15th harmonics were discarded in this paper.

The FMM–CART model received a total of 21 features, comprising the 1st, 5th, 7th, 11th, 13th, 17th, and 19th harmonics from phase current A, phase current B, and phase current C. All the input data were normalized between 0 and 1. The output of FMM–CART was the prediction of the motor condition, with class 1 indicating a healthy motor, classes 2–5 indicating a motor with broken rotor bars, unbalanced voltages, stator winding faults, and eccentricity problems, respectively.

Note that when a small data set is used, the prediction error estimate could vary from one run to another, and the presence of an outlier could change the prediction error estimate considerably [68]. In this regard, the cross-validation method allows a better estimate of the prediction error [68]. Hence, the k-fold ($k = 5$) cross-validation method was adopted in this paper. As such, the experiment was repeated five times, each time the motor was operated at 25%, 50%, 75%, and 100% load conditions. The results (averages and standard deviations) were computed using the bootstrap method [69] with 5000 resamplings. Using an Intel Core2 Duo 2.80 GHz processor with 4 GB RAM on MATLAB R2010a, the computational time taken by a single run of the cross-validation experiment was also recorded.

1) Broken Rotor Bars: The induction motor was operated with first one broken bar and then two broken bars. Table III shows the overall results. FMM–CART and CART produced stable results at 100% accuracy. FMM, with 98.41% accuracy, produced the most complex network structure with 10

TABLE III
FMM, CART, AND FMM–CART RESULTS FOR BROKEN ROTOR BARS

Network	Accuracy (%)	Std. Dev.	Complexity	Time (sec)
FMM	98.41	2.58	10 hyperboxes	0.11
CART	100.00	0.00	2 leafs	0.86
FMM–CART	100.00	0.00	2 leafs	0.94

TABLE IV
FMM, CART, AND FMM–CART RESULTS FOR UNBALANCED VOLTAGE

Network	Accuracy (%)	Std. Dev.	Complexity	Time (sec)
FMM	96.70	4.18	7 hyperboxes	0.11
CART	100.00	0.00	2 leafs	0.92
FMM–CART	100.00	0.00	2 leafs	0.94

hyperboxes, while CART and FMM–CART contained only 2 leafs. Nevertheless, the computational time of FMM was only 0.11 s, while CART and FMM–CART consumed close to 1 s. From the analysis of CART and FMM–CART, the most significant feature detected was the 5th harmonic of phase B. This is in line with the finding in [70], that is, the 5th harmonic amplitudes differ when comparing a healthy motor with one that has broken rotor bars. In [71], it has also been stated that the 5th harmonic is a good indicator for broken rotor bars.

In [36], the WPD method was used to extract different frequency resolutions while MLP with BP was used for fault detection based on stator currents. Motors with one and two broken rotor bars were analyzed. In [37], MDA was used to detect broken rotor bars too. The best results of WPD with MLP and MDA (extracted from [36], [37]) are comparable with those of FMM–CART, with 99% and 99.38% accuracy, respectively. Nevertheless, batch learning was used in WPD with MLP [36], while one-pass learning was realized in FMM–CART. Thus, FMM–CART enjoys the advantage of a single-pass training scheme over WPD with MLP in its operation.

2) Unbalanced Voltages: The induction motor was operated by biasing one of three-phase unbalanced voltages by first 5%, followed by 10%. Table IV shows the results. FMM produced 96.7% accuracy, while CART and FMM–CART achieved stable results at 100% accuracy. Again, the structure of FMM was the most complex with seven hyperboxes while CART and FMM–CART contained only two leafs. The computational time of FMM was only 0.11 s while CART and FMM–CART consumed almost 1 s. The most significant feature from CART and FMM–CART was the 13th harmonic of phase A. Sharifi and Ebrahimi [72] took the 13th harmonic into consideration as there was a significant magnitude change when comparing a healthy motor with one that has unbalanced supply.

In [17], FFT was used for processing signals from machine voltage, current, speed, vibration, and temperature. The outputs of FFT were fed to an MLP network with BP learning. The network achieved 100% accuracy for unbalanced voltage detection. In comparison with this paper in [17] which used five different inputs, FMM–CART exhibits the advantage that its input is only from a single source, that is, the stator currents of induction motors.

3) Stator Winding Faults: In this test, the induction motor was operated with 10% turn shorts in one of the three phases having stator windings short. Table V shows the results. Again, FMM produced the lowest accuracy rate with the most complex network structure, but with the shortest computational time. The results of CART and FMM–CART are similar. The most significant feature from CART and FMM–CART was the 5th harmonic of phase A, that is, the same as in eccentricity problems. In [73], it is shown that the 5th harmonic of the current spectrum changes when comparing a healthy motor with one that has inter-turn stator winding faults.

In [16], ANFIS was used to classify inter-turn insulation faults. The test was conducted using a single-phase induction motor. Two tests were performed: first with two inputs (speed and current) and second with five inputs (speed, current, winding temperature, bearing temperature, and machine noise). The inputs were transformed using FFT and then fed into ANFIS. In [74], a fuzzy system with inputs generated by the finite element method was used to classify stator winding faults. Based on two and five inputs, ANFIS [16] achieved 94.03% and 96.67% accuracy, respectively. The fuzzy system produced 100% accuracy [74]. Comparatively, FMM–CART used only one input source, that is, the stator currents of induction motors. This shows the ability of FMM–CART to produce a high accuracy rate with minimal input information when compared to ANFIS.

4) Eccentricity Problems: The induction motor was operated under the condition of both dynamic and static eccentricity. In accordance with [11], mixed dynamic and static eccentricity was obtained by fitting nonconcentric support parts between the shaft and bearing, as in Fig. 4(c). In this paper, 30% dynamic eccentricity and 10% static eccentricity were produced for evaluation. Table VI shows the results. Similar performance trends as in the previous experiments could be observed. The most significant feature from CART and FMM–CART was the 5th harmonic of phase A. This is in line with the finding of Faiz *et al*. [70] where the current spectrum analysis showed that the 5th harmonic amplitude differs when comparing a healthy motor with one that has static eccentricity. Cusido *et al*. [75] noted that rotor eccentricity faults are visible specifically around the 5th harmonic.

In [46], two air-gap eccentricity tests were performed. Vibration signals were used as inputs to short-time fourier transform (STFT) for processing. The output of STFT, that is, vibration spectra, was fed into an MLP network. In [11], the same method was used with current signals fed into a predictive filter using FFT. The results were between 97% and 100% accuracy for STFT–MLP [46], and 92% accuracy for the predictive filter with FFT. Comparatively, FMM–CART is able to yield similar, if not better, performance as compared with STFT–MLP and the predictive filter with FFT.

C. Multiple Induction Motors Faults

From the results in the previous section, it is evident that FMM–CART is able to perform well in comparison with different methods reported in the literature for detection and diagnosis of individual induction motor faults. Nevertheless,

TABLE V
FMM, CART, AND FMM–CART RESULTS FOR STATOR WINDING FAULTS

Network	Accuracy (%)	Std. Dev.	Complexity	Time (sec)
FMM	97.59	3.35	6 hyperboxes	0.10
CART	100.00	0.00	2 leafs	0.89
FMM–CART	100.00	0.00	2 leafs	0.93

TABLE VI
FMM, CART, AND FMM–CART RESULTS FOR BROKEN ROTOR BARS

Network	Accuracy (%)	Std. Dev.	Complexity	Time (sec)
FMM	98.79	1.96	6 hyperboxes	0.10
CART	100.00	0.00	2 leafs	0.91
FMM–CART	100.00	0.00	2 leafs	0.96

it would be useful if FMM–CART could detect and diagnose different types of induction motor faults. As such, an additional test was conducted with four fault conditions combined together. This is an important and comprehensive induction motor fault detection and diagnosis study using inputs from only a single source (i.e., stator current signals), as thus far, most of the researches have been confined to either single or multiple fault conditions with multiple input sources, as discussed in Section II.

To evaluate the robustness of FMM–CART, two sets of experiments (one with noise and one without) have been conducted. The results are compared with those from FMM and CART. Statistical analysis using the bootstrap hypothesis tests has also been performed. The details are as follows.

1) Inputs without Noise: Table VII shows a summary of the overall accuracy rates of five motor conditions (healthy, broken rotor bars, unbalanced voltages, eccentricity, and stator winding faults) using FMM, CART, and FMM–CART.

As can be seen, FMM produced the lowest accuracy of 93.62%, while CART and FMM–CART achieved 98.11% and 98.25% accuracy for multiple motor conditions. In FMM–CART, the hyperboxes resulted from FMM training compressed the number of original data samples to only 12%. These data samples were used by FMM–CART to produce the best accuracy of 98.25%. The decision tree produced by FMM–CART is the same as that of CART. This implies that, in FMM–CART, FMM is useful for extracting the important features for subsequent classification by CART. A decision tree resulting from FMM–CART showing all motor conditions is depicted in Fig. 5.

Analysis of the decision tree for all motor conditions is as follows. First, note that the relative importance is a crucial indicator, which sums across all nodes in a tree and allows ranking of different inputs as well as identifying the significant variables in the feature set. Based on the tree shown in Fig. 5, the 5th harmonic is useful for detecting eccentricity problems, broken rotor bars, and stator winding faults while the 13th harmonic is useful for detecting unbalanced voltages. The tree starts by splitting the 5th harmonic of phase A, which is the most significant feature in the tree with a relative importance of 100%. If the value of the 5th harmonics of phase A is smaller than 0.5625, FMM–CART classifies the input as eccentricity problems. Otherwise, splitting is needed at the 5th harmonic of phase B (the second most important feature with a relative importance of 61.7%). If the value of the 5th harmonic of phase B is larger than 0.5806, FMM–CART classifies the input as broken rotor bars. Otherwise, splitting occurs again at the 5th harmonic of phase A. If the value of the 5th harmonic of phase A is larger than 0.5872, FMM–CART classifies the input as stator winding faults. Otherwise, splitting happens at the 13th harmonic of phase A (the third most important feature with a relative importance of 36.6%). Unbalanced voltages are detected if the value of the 13th harmonic of phase A is smaller than 0.4426. Otherwise, the input is predicted to be from a healthy motor.

TABLE VII
FMM, CART, AND FMM–CART RESULTS FOR FIVE MOTOR CONDITIONS

Network	Accuracy (%)	Std. Dev.	Complexity	Time (sec)
FMM	93.62	3.39	18 hyperboxes	0.21
CART	98.11	1.36	5 leafs	0.92
FMM–CART	98.25	1.20	5 leafs	0.96

TABLE VIII
FMM–CART RESULTS WITH NOISY SIGNALS

Noise (%)	Network	Accuracy (%)	Std. Dev.	Complexity	Time (sec)
10	FMM	90.51	4.19	18 hyperboxes	0.23
	CART	95.15	2.16	5 leafs	0.95
	FMM–CART	95.78	1.87	5 leafs	1.02
20	FMM	86.86	5.95	20 hyperboxes	0.26
	CART	91.67	3.92	6 leafs	0.97
	FMM–CART	93.00	3.30	6 leafs	1.05
30	FMM	81.81	6.82	21 hyperboxes	0.27
	CART	86.86	4.79	7 leafs	0.98
	FMM–CART	89.30	3.99	6 leafs	1.03
40	FMM	70.87	7.30	23 hyperboxes	0.26
	CART	76.44	5.27	8 leafs	1.01
	FMM–CART	81.58	4.37	7 leafs	1.06
50	FMM	58.31	7.61	24 hyperboxes	0.28
	CART	64.48	5.58	8 leafs	1.02
	FMM–CART	73.04	4.61	7 leafs	1.08

2) Inputs with Noise: To further evaluate the effectiveness of all three models, the test samples were corrupted with white Gaussian noise from 10% to 50%. The channel powers of the noise-corrupted test samples were measured, and a 20 dB signal-to-noise ratio was added individually. All noise-corrupted test samples were normalized between 0 and 1. Table VIII shows the overall results.

The performance of FMM–CART was relatively stable with up to 20% noisy test samples. However, the performances of FMM–CART deteriorated when more test samples were corrupted by noise, and the tree grew bigger in line with

TABLE IX
PERFORMANCE COMPARISON OF FMM–CART WITH FMM AND CART USING BOOTSTRAP HYPOTHESIS TEST

Noise (%)		0	10	20	30	40	50	0	10	20	30	40	50
Model	Y	FMM						CART					
	X	FMM–CART						FMM–CART					
p-value		0.003	0.004	0.011	0.010	0.002	0.001	0.403	0.257	0.224	0.129	0.023	0.003

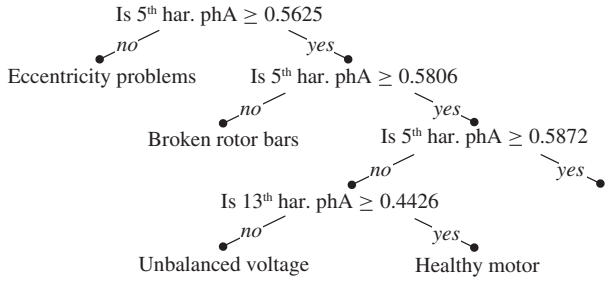

Fig. 5. Decision tree for all motor conditions.

increasing noise levels. When the noise level increased from 30% to 50%, the tree structure of CART became more complicated than that of FMM–CART.

In [14], three-phase line voltages and currents were used as inputs to FFT and to WPD. The outputs, that is, the fundamental and harmonic components, were then fed into a recurrent NN model for fault detection and diagnosis. An accuracy of 93% was achieved for classifying three fault conditions, that is, broken rotor bars, stator winding turn short, and eccentricity. This indicates that FMM–CART is able to yield a higher accuracy rate than the recurrent NN model even with an extra fault condition (i.e., unbalanced voltages) included.

In terms of computational time, that consumed by FMM–CART was slightly over 1 s. As stated in [34], the wavelet-based SVM which used start-up transient currents to detect bowed rotors, broken rotor bars, eccentricity, bearing faults, mass and phase unbalanced voltages, and normal condition took 70.9–82.4 s for computation. This implies that FMM–CART is able to make predictions for multiple motor conditions quickly and accurately.

3) Hypothesis Tests: To further compare the results of FMM, CART, and FMM–CART statistically, the bootstrap hypothesis test [69], [76] with a significance level of 0.05 was conducted. One advantage of the bootstrap method is that it does not require the data samples to follow a normal distribution. The p-values of the corresponding tests are shown in Table IX. Referring to Table IX, the null hypothesis claims that the performances of models X and Y are equivalent, while the alternative hypothesis claims that model X performs better than model Y. It is observed that all p-values of FMM–CART as compared with FMM are smaller than 0.05, hence rejecting the null hypothesis. When FMM–CART is compared with CART, the p-values are lower than 0.05 for 40% and 50% noise levels. This indicates that FMM–CART performs better than both FMM (for 0% to 50% noise levels) and CART (for 40% to 50% noise levels) statistically at the 95% confidence limit. The hypothesis test results vindicate the robustness and usefulness of FMM–CART for induction motor fault detection and diagnosis in noisy environments.

VI. CONCLUSION

In this paper, a hybrid FMM–CART model for induction motor fault detection and diagnosis has been described. MCSA has been used for stator-current signal acquisition, and the current signals have been transformed into their frequency spectra. The resulting motor current harmonics have been employed to form the input features to FMM–CART for detection and diagnosis of individual and multiple motor fault conditions. The results of FMM–CART are comparable, if not better, than those from FMM, CART, as well as other methods reported in the literature. One of the important contributions of this paper is that, in addition to individual faults, five different motor conditions have been combined for fault detection and diagnosis using FMM–CART. This is a comprehensive study of induction motor fault diagnosis, and promising results with 98.25% accuracy in noise-free conditions have been achieved. FMM–CART also has been shown to perform well in noisy environments when compared with FMM and CART. In summary, FMM–CART is able to make rapid (slightly more than one second) and accurate (98.25% accuracy for five motor conditions in noise-free conditions) predictions for induction motor fault detection and diagnosis. Further work will focus on the implementation of MCSA and FMM–CART for real-time fault detection and diagnosis of induction motors.

REFERENCES

[1] A. Siddique, G. S. Yadava, and B. Singh, "A review of stator fault monitoring techniques of induction motors," *IEEE Trans. Energy Conv.*, vol. 20, no. 1, pp. 106–114, Mar. 2005.

[2] E. J. Wiedenbrug, A. Ramme, E. Matheson, A. Jouanne, and A. K. Wallace, "Modern online testing of induction motors for predictive maintenance and monitoring," *IEEE Trans. Ind. Appl.*, vol. 38, no. 5, pp. 1466–1472, Sep.–Oct. 2002.

[3] F. C. Trutt, J. Sottile, and J. L. Kohler, "Online condition monitoring of induction motors," *IEEE Trans. Ind. Appl.*, vol. 38, no. 6, pp. 1627–1632, Nov.–Dec. 2002.

[4] J. R. Millan-Almaraz, R. J. Romero-Troncoso, L. M. Contreras-Medina, and A. Garcia-Perez, "Embedded FPGA based induction motor monitoring system with speed drive fed using multiple wavelet analysis," in *Proc. Int. Symp. Ind. Embedded Syst.*, Jul. 2008, pp. 215–220.

[5] J. Cusidó, L. Romeral, J. A. Ortega, J. A. Rosero, and A. G. Espinosa, "Fault detection in induction machines using power spectral density in wavelet decomposition," *IEEE Trans. Ind. Electron.*, vol. 55, no. 2, pp. 633–643, Feb. 2008.

[6] M. Montanari, S. M. Peresada, C. Rossi, and A. Tilli, "Speed sensorless control of induction motors based on a reduced-order adaptive observer," *IEEE Trans. Control Syst. Technol.*, vol. 15, no. 6, pp. 1049–1064, Nov. 2007.

[7] A. T. de Almeida, *Energy Using Product (EuP) Directive Preparatory Study, Lot 11: Motors, Analysis of Existing Technical and Market Information*. Brussels, Belgium: DG TREN, Jun. 2006.

[8] *European Integral Horsepower Motors Markets*, Frost & Sullivan, Singapore, May 2003.

[9] *Commission of the European Communities, Full Impact Assessment*, Standard 1014, Jul. 2009.

[10] IAS Motor Reliability Working Group, "Report of large motor reliability survey of industrial and commercial installations, part I," *IEEE Trans. Ind. Appl.*, vol. 21, no. 4, pp. 853–864, Jul. 1985.

[11] P. V. J. Rodríguez, M. Negrea, and A. Arkkioa, "A simplified scheme for induction motor condition monitoring," *Mech. Syst. Signal Process.*, vol. 22, no. 5, pp. 1216–1236, 2008.

[12] W. T. Thomson and M. Fenger, "Current signature analysis to detect induction motor faults," *IEEE Trans. Ind. Appl.*, vol. 7, no. 4, pp. 26–34, Jul.–Aug. 2001.

[13] M. E. H. Benbouzid, M. Viera, and C. Theys, "Induction motor's fault detection and localization using stator-current advanced signal processing techniques," *IEEE Trans. Power Electron.*, vol. 14, no. 1, pp. 14–22, Jan. 1999.

[14] K. Kim, A. G. Parlos, and R. M. Bharadwaj, "Sensorless fault diagnosis of induction motors," *IEEE Trans. Ind. Electron.*, vol. 50, no. 5, pp. 1038–1051, Oct. 2003.

[15] H. Douglas, P. Pillay, and A. K. Ziarani, "Broken rotor bar detection in induction machines with transient operating speeds," *IEEE Trans. Energy Conver.*, vol. 20, no. 1, pp. 135–141, Mar. 2005.

[16] M. S. Ballal, Z. J. Khan, H. M. Suryawanshi, and R. L. Sonolikar, "Adaptive neural fuzzy inference system for the detection of inter-turn insulation and bearing wear faults in induction motor," *IEEE Trans. Ind. Electron.*, vol. 54, no. 1, pp. 250–258, Feb. 2007.

[17] G. K. Singh and S. A. S. A. Kazzaz, "Development of an intelligent diagnostic system for induction machine health monitoring," *IEEE Syst. J.*, vol. 2, no. 1, pp. 273–288, Jun. 2008.

[18] H. Arabacı and O. Bilgin, "Automatic detection and classification of rotor cage faults in squirrel cage induction motor," *Neural Comput. Appl.*, vol. 19, no. 5, pp. 713–723, Jul. 2010.

[19] Q. Guo, X. Li, H. Yu, W. Hu, and J. Hu, "Broken rotor bars fault detection in induction motors using Park's vector modulus and FWNN approach," in *Advances in Neural Networks*, vol. 5264. New York: Springer-Verlag, Sep. 2008, pp. 809–821.

[20] O. Ondela, E. Boutleuxa, G. Clercb, and E. Blanco, "FDI based on pattern recognition using Kalman prediction: Application to an induction machine," *Eng. Appl. Artif. Intell.*, vol. 21, no. 7, pp. 961–973, Oct. 2008.

[21] E. C. C. Lau and H. W. Ngan, "Detection of motor bearing outer raceway defect by wavelet packet transformed motor current signature analysis," *IEEE Trans. Instrum. Meas.*, vol. 59, no. 10, pp. 2683–2690, Oct. 2010.

[22] M. Riera-Guasp, M. F. Cabanas, J. A. Antonino-Daviu, M. Pineda-Sánchez, and C. H. R. García, "Influence of nonconsecutive bar breakages in motor current signature analysis for the diagnosis of rotor faults in induction motors," *IEEE Trans. Energy Conv.*, vol. 25, no. 1, pp. 80–89, Mar. 2010.

[23] S. Abe and M. S. Lan, "A method for fuzzy rules extraction directly from numerical data and its application to pattern classification," *IEEE Trans. Fuzzy Syst.*, vol. 3, no. 1, pp. 18–28, Feb. 1995.

[24] S. Abe and M. S. Lan, "Fuzzy rules extraction directly from numerical data for function approximation," *IEEE Trans. Syst., Man, Cybern.*, vol. 25, no. 1, pp. 119–129, Jan. 1995.

[25] G. I. S. Palmero, J. J. Santamariaa, E. J. M. Torrea, and J. R. P. González, "Fault detection and fuzzy rule extraction in AC motors by a neuro-fuzzy ART-based system," *Eng. Appl. Artif. Intell.*, vol. 18, no. 7, pp. 867–874, Oct. 2005.

[26] H. S. Sii, T. Ruxton, and J. Wang, "A fuzzy-logic-based approach to qualitative safety modeling for marine systems," *Rel. Eng. Syst. Safety*, vol. 73, no. 1, pp. 19–34, 2001.

[27] T. Brotherton, G. Chadderdon, and P. Grabill, "Automated rule extraction for engine vibration analysis," in *Proc. Aerosp. Conf.*, vol. 3. Mar. 1999, pp. 29–39.

[28] V. T. Tran, B. S. Yang, M. S. Oh, and A. C. C. Tan, "Fault diagnosis of induction motor based on decision trees and adaptive neuro-fuzzy inference," *Expert Syst. Appl.*, vol. 36, no. 2, pp. 1840–1849, Mar. 2009.

[29] P. K. Simpson, "Fuzzy min-max neural networks. I. Classification," *IEEE Trans. Neural Netw.*, vol. 3, no. 5, pp. 776–786, Sep. 1992.

[30] L. Breiman, J. H. Friedman, R. A. Olshen, and C. J. Stone, *Classification and Regression Trees*. Belmont, CA: Chapman & Hall, 1984.

[31] H. A. Talebi, K. Khorasani, and S. Tafazoli, "A recurrent neural-network-based sensor and actuator fault detection and isolation for nonlinear systems with application to the satellite's attitude control subsystem," *IEEE Trans. Neural Netw.*, vol. 20, no. 1, pp. 45–60, Jan. 2009.

[32] S. Huang and K. K. Tan, "Fault detection and diagnosis based on modeling and estimation methods," *IEEE Trans. Neural Netw.*, vol. 20, no. 5, pp. 872–881, May 2009.

[33] S. H. Lee, Y. G. Wang, and J. I. Song, "Fourier and wavelet transformations application to fault detection of induction motor with stator-current," *J. Cent. South Univ. Technol.*, vol. 17, pp. 93–101, Feb. 2010.

[34] A. Widodo and B. S. Yang, "Wavelet support vector machine for induction machine fault diagnosis based on transient current," *Expert Syst. Appl.*, vol. 35, nos. 1–2, pp. 307–316, Jul. 2008.

[35] T. Han, B. S. Yang, and Z. J. Yin, "Feature-based fault diagnosis system of induction motors using vibration signal," *J. Qual. Maint. Eng.*, vol. 13, no. 2, pp. 163–175, 2007.

[36] A. Sadeghian, Z. Ye, and B. Wu, "Online detection of broken rotor bars in induction motors by wavelet packet decomposition and artificial neural networks," *IEEE Trans. Instrum. Meas.*, vol. 58, no. 7, pp. 2253–2263, Jul. 2009.

[37] B. Ayhan, M. Y. Chow, and M. H. Song, "Multiple signature processing-based fault detection schemes for broken rotor bar in induction motors," *IEEE Trans. Energy Conv.*, vol. 20, no. 2, pp. 336–343, Jun. 2005.

[38] Y. Lei, Z. He, and Y. Zi, "A new approach to intelligent fault diagnosis of rotating machinery," *Expert Syst. Appl.*, vol. 35, no. 4, pp. 1593–1600, Nov. 2008.

[39] L. Zhang, G. Xiong, H. Liu, H. Zou, and W. Guo, "Bearing fault diagnosis using multi-scale entropy and adaptive neuro-fuzzy inference," *Expert Syst. Appl.*, vol. 37, no. 8, pp. 6077–6085, Aug. 2010.

[40] Y. R. Hwang, K. K. Jen, and Y. T. Shen, "Application of cepstrum and neural network to bearing fault detection," *J. Mech. Sci. Technol.*, vol. 23, no. 10, pp. 2730–2737, May 2009.

[41] I. Y. Önel, E. Ayçiçek, and I. Senol, "An experimental study, about detection of bearing defects in inverter fed small induction motors by Concordia transform," *J. Intell. Manuf.*, vol. 20, no. 2, pp. 243–247, Jan. 2009.

[42] Z. Xu, J. Xuan, T. Shi, B. Wu, and Y. Hu, "A novel fault diagnosis method of bearing based on improved fuzzy ARTMAP and modified distance discriminant technique," *Expert Syst. Appl.*, vol. 36, no. 9, pp. 11801–11807, Nov. 2009.

[43] B. Samanta and C. Nataraj, "Application of particle swarm optimization and proximal support vector machines for fault detection," *Swarm Intell.*, vol. 3, no. 4, pp. 303–325, May 2009.

[44] V. N. Ghate and S. V. Dudul, "Cascade neural network based fault classifier for three phase induction motor," *IEEE Trans. Ind. Electron.*, vol. 58, no. 5, pp. 1555–1563, May 2011.

[45] V. F. Pires, J. F. Martins, and A. J. Pires, "Eigenvector/eigenvalue analysis of a 3-D current referential fault detection and diagnosis of an induction motor," *Energy Conver. Manage.*, vol. 51, no. 5, pp. 901–907, May 2010.

[46] H. Su and K. T. Chong, "Induction machine condition monitoring using neural network modeling," *IEEE Trans. Ind. Electron.*, vol. 54, no. 1, pp. 241–249, Feb. 2007.

[47] N. T. Nguyen, H. H. Lee, and J. M. Kwon, "Optimal feature selection using genetic algorithm for mechanical fault detection of induction motor," *J. Mech. Sci. Technol.*, vol. 22, no. 3, pp. 490–496, Sep. 2008.

[48] H. C. Cho, J. Knowles, M. S. Fadali, and K. S. Lee, "Fault detection and isolation of induction motors using recurrent neural networks and dynamic Bayesian modeling," *IEEE Trans. Control Syst. Technol.*, vol. 18, no. 2, pp. 430–437, Mar. 2010.

[49] X. Liu, L. Ma, and J. Mathew, "Machinery fault diagnosis based on fuzzy measure and fuzzy integral data fusion techniques," *Mech. Syst. Signal Process.*, vol. 23, no. 3, pp. 690–700, 2009.

[50] M. B. K. Bouzid, G. Champenois, N. M. Bellaaj, L. Signac, and K. Jelassi, "An effective neural approach for the automatic location of stator interturn faults in induction motor," *IEEE Trans. Ind. Electron.*, vol. 55, no. 12, pp. 4277–4289, Dec. 2008.

[51] H. Taplak, I. Uzmay, and S. Yildirim, "An artificial neural network application to fault detection of a rotor bearing system," *Ind. Lubricat. Tribol.*, vol. 58, no. 1, pp. 32–44, 2006.

[52] G. Niu, S. S. Lee, B. S. Yang, and S. J. Lee, "Decision fusion system for fault diagnosis of elevator traction machine," *J. Mech. Sci. Technol.*, vol. 22, no. 1, pp. 85–95, Jul. 2008.

[53] M. A. Awadallah and M. M. Morcos, "Application of AI tools in fault diagnosis of electrical machines and drives-an overview," *IEEE Trans. Energy Conserv.*, vol. 18, no. 2, pp. 245–251, Jun. 2003.

[54] *National Electrical Manufacturers Association*, NEMA Standard MG 1-2009, 2009.

[55] D. G. Dorrell, W. T. Thomson, and S. Roach, "Analysis of airgap flux, current, and vibration signals as a function of the combination of static and dynamic airgap eccentricity in 3-phase induction motors," *IEEE Trans. Ind. Appl.*, vol. 33, no. 1, pp. 24–34, Jan.–Feb. 1997.
[56] J. Penman, H. G. Sedding, B. A. Lloyd, and W. T. Fink, "Detection and location of interturn short circuits in the stator windings of operating motors," *IEEE Trans. Energy Conv.*, vol. 9, no. 4, pp. 652–658, Dec. 1994.
[57] G. M. Joksimovic and J. Penman, "The detection of inter-turn short circuits in the stator winding of operating motors," *IEEE Trans. Ind. Appl.*, vol. 47, no. 5, pp. 1078–1084, Oct. 2000.
[58] M. Haji and H. A. Toliyat, "Pattern recognition-a technique for induction machines rotor broken bar detection," *IEEE Trans. Energy Conv.*, vol. 16, no. 4, pp. 312–317, Dec. 2001.
[59] J. R. Cameron, W. T. Thomson, and A. B. Dow, "Vibration and current monitoring for detecting airgap eccentricity in large induction motors," *IEE Proc. Electr. Power Appl.*, vol. 133, no. 3, pp. 155–163, May 1986.
[60] P. Herman, G. Prasad, T. M. McGinnity, and D. Coyle, "Comparative analysis of spectral approaches to feature extraction for EEG-based motor imagery classification," *IEEE Trans. Neural Syst. Rehabil. Eng.*, vol. 16, no. 4, pp. 317–326, Aug. 2008.
[61] P. K. Simpson, "Fuzzy min-max neural networks – Part 2: Clustering," *IEEE Trans. Fuzzy Syst.*, vol. 1, no. 1, pp. 32–45, Feb. 1993.
[62] B. Gabrys and A. Bargiela, "General fuzzy min-max neural network for clustering and classification," *IEEE Trans. Neural Netw.*, vol. 11, no. 3, pp. 769–783, May 2000.
[63] A. V. Nandedkar and P. K. Biswas, "A fuzzy min-max neural network classifier with compensatory neuron architecture," *IEEE Trans. Neural Netw.*, vol. 18, no. 1, pp. 42–53, Jan. 2007.
[64] A. V. Nandedkar and P. K. Biswas, "A granular reflex fuzzy min–max neural network for classification," *IEEE Trans. Neural Netw.*, vol. 20, no. 7, pp. 1117–1134, Jul. 2009.
[65] H. Daniels and M. Velikova, "Monotone and partially monotone neural networks," *IEEE Trans. Neural Netw.*, vol. 21, no. 6, pp. 906–917, Jun. 2010.
[66] R. J. Lewis, *An Introduction to Classification and Regression Tree (CART) Analysis*. San Francisco, CA: Society Academic Emergency Medicine, 2000.
[67] J. Pedra, L. Sainz, and F. Córcoles, "Harmonic modeling of induction motors," *Electr. Power Syst. Res.*, vol. 76, pp. 936–944, Jul. 2006.
[68] F. Altiparmak, B. Dengiz, and A. E. Smith, "A general neural network model for estimating telecommunications network reliability," *IEEE Trans. Rel.*, vol. 58, no. 1, pp. 2–9, Mar. 2009.
[69] B. Efron, "Bootstrap methods: Another look at the jackknife," *Ann. Stat.*, vol. 7, no. 1, pp. 1–26, Jan. 1979.
[70] J. Faiz, B. M. Ebrahimi, H. A. Toliyat, and W. S. Abu-Elhaija, "Mixed-fault diagnosis in induction motors considering varying load and broken bars location," *Energy Conv. Manage.*, vol. 51, no. 7, pp. 1432–1441, Jul. 2010.
[71] C. Bruzzese and E. Santini, "Experimental performances of harmonic current sideband based broken bar indicators," in *Proc. IEEE Int. Symp. Diag. Electr. Mach. Power Electron. Drives*, Nov. 2007, pp. 226–230.
[72] R. Sharifi and M. Ebrahimi, "Detection of stator winding faults in induction motors using three-phase current monitoring," *ISA Trans.*, vol. 50, no. 1, pp. 14–20, Jan. 2011.
[73] Y. Amara and G. Barakat, "Modeling and diagnostic of stator faults in induction machines using permeance network method," in *Proc. Electromag. Res. Symp.*, Mar. 2011, pp. 1550–1559.
[74] P. V. J. Rodríguez and A. Arkkio, "Detection of stator winding fault in induction motor using fuzzy logic," *Appl. Soft Comput.*, vol. 8, pp. 1112–1120, Mar. 2008.
[75] J. Cusido, J. Rosero, E. Aldabas, J. A. Ortega, and L. Romeral, "Fault detection techniques for induction motors," in *Proc. IEEE Compat. Power Electron.*, Jun. 2005, pp. 85–90.
[76] P.I. Good, *Permutation, Parametric and Bootstrap Tests of Hypotheses*. Huntington Beach, CA: Springer-Verlag, 2005.

Manjeevan Seera (M'11) received the B.E. degree in electrical and electronics engineering from the University of Sunderland, Sunderland, U.K., in 2007. He is currently pursuing the Ph.D. degree with the School of Electrical and Electronic Engineering, University of Science Malaysia, Nibong Tebal, Malaysia.

His current research interests include soft computing, fault detection, diagnosis, and printed circuit board designs.

Chee Peng Lim received the B.E. degree in electrical engineering from the University of Technology, Permatang Pauh, Malaysia, the M.Sc. degree in engineering control systems, and the Ph.D. degree from the University of Sheffield, Sheffield, U.K., in 1992, 1993, and 1997, respectively.

He has published more than 150 papers in books, international journals, and conference proceedings. His current research interests include soft computing, pattern recognition, medical prognosis, fault detection and diagnosis, and condition monitoring.

Dahaman Ishak received the B.E. degree from the University of Syracuse, Syracuse, NY, the M.Sc. degree from the University of Newcastle upon Tyne, Newcastle, U.K., and the Ph.D. degree from the University of Sheffield, Sheffield, U.K., all in electrical engineering, in 1990, 2001, and 2005, respectively.

He is currently a Senior Lecturer with the School of Electrical and Electronic Engineering, University of Science Malaysia, Nibong Tebal, Malaysia. His current research interests include the design and analysis of low-speed high-torque permanent-magnet brushless machines, electrical drives, and research on renewable energy.

Harapajan Singh received the M.Sc. degree in electrical power and control from the University of Nottingham, Nottingham, U.K., in 1989.

He is a Professional Electrical Engineer and Competent Electrical Engineer registered with the Energy Commission. He is currently a Senior Lecturer with the Faculty of Electrical Engineering, Universiti Teknologi MARA, Permatang Pauh, Malaysia. His current research interests include fault detection and diagnosis, power quality, and energy management.

Mr. Singh received the Engineering Council Part II, London, U.K., in 1983.